Article

Tidal Effects and Clock Comparison Experiments

Cheng-Gang Qin, Tong Liu, Jin-Zhuang Dong, Xiao-Yi Dai, Yu-Jie Tan and Cheng-Gang Shao

Article

Tidal Effects and Clock Comparison Experiments

Cheng-Gang Qin [1], Tong Liu [2], Jin-Zhuang Dong [1], Xiao-Yi Dai [1], Yu-Jie Tan [1] and Cheng-Gang Shao [1,*]

1   MOE Key Laboratory of Fundamental Physical Quantities Measurement and Hubei Key Laboratory of Gravitation and Quantum Physics, PGMF and School of Physics, Huazhong University of Science and Technology, Wuhan 430074, China

2   Key Laboratory of Space Utilization, Technology and Engineering Center for Space Utilization, Chinese Academy of Sciences, Beijing 100094, China

*   Correspondence: cgshao@hust.edu.cn

Abstract: Einstein's general relativity theory provides a successful understanding of the flow of time in the gravitational field. From Einstein's equivalence principle, the influence of the Sun and Moon masses on clocks is given in the form of tidal potentials. Two clocks fixed on the surface of the Earth, compared to each other, can measure the tidal effects of the Sun and Moon. The measurement of tidal effects can provide a test for general relativity. Based on the standard general relativity method, we rigorously derive the formulas for clock comparison in the Barycentric Celestial Reference System and Geocentric Celestial Reference System, and demonstrate the tidal effects on clock comparison experiments. The unprecedented performance of atomic clocks makes it possible to measure the tidal effects on clock comparisons. We propose to test tidal effects with the laboratory clock comparisons and some international missions, and give the corresponding estimations. By comparing the state-of-the-art clocks over distances of 1000 km, the laboratory may test tidal effects with a level of 1%. Future space missions, such as the China space station and FOCOS mission, can also be used to test tidal effects, and the best accuracy may reach 0.3%.

Keywords: tidal effects; clock comparison; equivalence principle; general relativity

1. Introduction

Einstein's general relativity (GR) theory is one of the deepest fundamental theories, which give the best description of the physical world at macroscopic scales. A central prediction of general relativity is the effect of gravitational redshift; clocks experience a frequency shift in a gravitational potential. Considering the Earth mass, a clock farther way from the Earth runs faster than a clock closer to the Earth. By using precision clocks in the Earth gravitational field, the gravitational redshift has recently been accurately tested with Galileo satellites [1,2] and the Tokyo tower [3]. Considering the masses of the Sun and Moon, clocks experience a different frequency shift, which is not proportional to the gravitational potentials and is different to the Earth case. From the equivalence principle, in a local coordinate system, the influence of external matter should be given by the tidal potentials, and the intrinsic effects of external matter is the inhomogeneous gravitational field [4,5]. For the clock comparison in the vicinity of the Earth, it does not display a frequency shift due to the Sun's and Moon's gravitational potentials at the first order $\Delta U_{S/M}/c^2$, and the experimental outcomes are the tidal effects of the Sun and Moon masses. Experimental confirmation of the gravitational effects of the Sun and Moon is as necessary as the gravitational redshift of the Earth mass. The measurement of tidal effects on clock comparison is important both for general relativity and the equivalence principle. Although tidal effects on clocks are weak compared with the Earth's gravitational redshift, the frequency shift due to the Sun's and Moon's tidal potentials is observable for today's best clocks. When comparing two clocks at a distance of about 1000 km, tidal effects can reach the level of 10^{-17} [6,7].

The test of the gravitational effect is mainly limited by the accuracy of the clocks. Sixty years after the first atomic clock, they have reached the unprecedented instability and uncertainty of the level of 10^{-18}, even 10^{-19} [8–13], and can provide the best available references for times and frequency. The developing performance gives a great prospect to precisely detect fundamental physical effects. Moreover, these clocks have widely been applied in the field of technology and science, such as the Global Positioning System (GPS) [14,15], relativistic geodesy [16,17], exploration of new physical effects [18–21], tests of Lorentz symmetry [22–25] and tests of fundamental constant variation [26–28]. For example, near the surface of the Earth, a fractional frequency shift of 1.1×10^{-18} corresponds to a height difference of 1 cm, and atomic clocks may be applied as next-generation geodetic tools. From a tower with 450 m height difference [3], frequency comparison between a pair of transportable optical clocks provides a high precision test for gravitational redshift. Another important example is to search new physics beyond the general relativity and standard model. An interesting topic is the Lorentz violation and CPT violation that lead to anisotropic spacetimes. The clock-comparison experiments search for the changes in the ticking rate of clocks on their orientation, which can display the corresponding properties of spacetime. Alan Kostelecký and colleagues, and many researchers have made numerous efforts in theories and experiments, and many infusive works have been reported [22–24,29–33]. In addition, by comparison experiments of the state-of-the-art clocks, it is possible to measure the tidal effects induced by the Sun and Moon masses. In the presence of Lorentz violation or CPT violation, the influence of the Sun's and Moon's masses is not just the tidal forms, and some new terms may appear.

The rapid development of clocks has motivated a number of international missions on orbiting clocks. The European Space Agency (ESA) project Space–Time Explorer and QUantum Equivalence Space Test (STE-QUEST) carries out tests of Einstein's equivalence principle using atomic clocks and long distance time/frequency links [34]. The Atomic Clock Ensemble in Space (ACES) project is scheduled to launch with cold atomic clocks [35]. A laser-cooled microwave clock operated on the China space station and there are plans to demonstrate an optical lattice clock in subsequent projects [36]. A space mission, fundamental physics with a state-of-the-art optical clock in space (FOCOS), plans to deploy an optical clock and a high stability laser link in space [37]. The GPS satellites carrying on-board atomic clocks can make the precise determination of position and timing. For these in-orbit clocks, tidal effects are more significant in high orbit and become measurable. These planned projects provide a possibility for measuring tidal effects of the Sun and Moon masses. In addition, the clock comparison with 1840 km optical fiber link has also been successfully demonstrated in laboratory with a level of 10^{-18} [38]. Although long distance clock comparisons are not sensitive to the test of gravitational redshift, they can provide a validation for tidal effects on clocks.

The paper is organized as follows. In Section 2, we discuss the clock comparisons and tidal effects in the framework of general relativity. In Section 2.1, we discuss the tidal effects of clock comparison in a freely falling elevator. By the method of general relativity, Sections 2.2 and 2.3 present a rigorous procedure to deduce the frequency shift for clock comparison experiments in the BCRS and GCRS, respectively. In Section 3, the test of tidal effects are estimated in the laboratory clock comparisons and some international space missions. The conclusion is given in Section 4.

2. Clock Comparisons in the General Relativity Reference Systems

The general relativity theory is a covariant theory where coordinate charts are just mathematical labels and physical measurements should be constructed as some coordinate-independent quantities [5,39]. It implies that different coordinate systems are equivalent and, for the considered experiments, one could choose an arbitrary coordinate system to model the measurements. For the purpose of actual calculations on the various experiments, different reference systems are indispensable. In the solar system, two coordinate reference systems, the solar system barycentric coordinate reference system (BCRS) and the geocen-

tric coordinate reference system (GCRS), are very useful, and are regarded as global and local reference systems. A reasonable choice of coordinate system can simplify the physical models. Usually, the local reference system may be of relevance for physical processes in the vicinity of the corresponding body, such as laser ranging to artificial satellites in the local environment of the Earth [5,40]. From the physical point of view, any reference system covering the region under consideration can be used to describe the physical quantities in that region; however, some reference systems can provide a simpler mathematical description for physical laws. They mean that the clock-comparison experiments in the laboratories can be appropriately described in both GCRS and BCRS. We show the equivalence of frequency shift of clock experiments between two reference systems and spurious coordinate effects vanish when we use GCRS to describe the clock comparisons.

For the clock comparison experiments in the vicinity of the Earth, the relativistic frequency shift can be deduced in both BCRS and GCRS. The influence of Earth mass is given by the gravitational potential, which leads to the well-known gravitational redshift. With a number of clock comparison experiments, gravitational redshift due to the Earth has been validated to the level of 10^{-5}. For the Sun's gravitational field, comparing two clocks on the equator distributed along the diameter of the Earth, *a priori* estimation indicates a gravitational redshift of 8×10^{-13}. However, this is essentially a "null redshift" in experimental outcome due to a cancellation from Doppler effects. It implies that the influence of Sun and Moon masses is not given in the form of gravitational potentials and the classic gravitational redshift is turned off in clock comparisons. In other words, clock comparisons on the Earth cannot display a frequency shift due to the first order in gravitational potential difference. This is sometimes called "*absence of the noon–midnight redshift*" [41], as an important consequence of the equivalence principle. We subsequently posit that the influence of the Sun and Moon masses is given in the form of tidal potentials, and tidal effects can never be turned off in clock comparisons.

2.1. Tidal Potentials and Clock Comparison

To demonstrate the tidal effects, we consider an Einstein elevator that is freely falling in the gravitational field of massive body GM. Compared to this massive body, the mass of the elevator is negligible. The gravitational field and gravitational acceleration of the position $\boldsymbol{r}$ can be expressed as GM/r and $-GM\boldsymbol{r}/r^3$, respectively (the origin of the coordinates is set at the center of mass of the massive body). Then two identical clocks A and B are fixed on the elevator with vertical height Δr. By using an electromagnetic signal, one can perform frequency comparison between clocks A and B, and the frequency difference of the two clocks can be characterized by frequency shift f_B/f_A. Firstly, we consider an observer measuring the frequency difference in the elevator. According to the equivalence principle, in the elevator the influence of the massive body is given in the form of tidal potentials and the frequency difference between the two clocks is caused by the difference of tidal potentials. If in a uniform gravitational field, the outcome of clock-comparison experiments cannot reveal the existence of external matter, and the frequency difference is 0. Then, we consider another observer fixed on this massive body. By a standard general relativity process, this frequency shift can be expressed as

$$\frac{f_B}{f_A} - 1 = -\frac{\boldsymbol{n}_{AB} \cdot (\boldsymbol{v}_B - \boldsymbol{v}_A)}{c} - \frac{1}{c^2}\left[\frac{v_A^2 - v_B^2}{2} + (\boldsymbol{n}_{AB} \cdot \boldsymbol{v}_A)(\boldsymbol{n}_{AB} \cdot \boldsymbol{v}_B) - (\boldsymbol{n}_{AB} \cdot \boldsymbol{v}_A)^2\right] - \frac{U_A - U_B}{c^2}, \qquad (1)$$

where c is the speed of light, $\boldsymbol{n}_{AB}$ is the uniter vector pointing from clock A to clock B, $\boldsymbol{v}_A$ is the velocity of clock A at the time of transmission, $\boldsymbol{v}_B$ is the velocity of clock B at the time of reception, r_A is the position of clock A at the time of transmission and r_B is the position of clock B at the time of reception. In this equation, the first two terms are Doppler effects and the third term is gravitational redshift caused by the massive body. For the frequency shift of order c^{-2}, the time interval of the signal from clocks A to B can be expressed as $\Delta r/c$ and the difference of coordinate velocity is given by $\boldsymbol{v}_B - \boldsymbol{v}_A = \boldsymbol{a}\Delta r/c$. $\boldsymbol{a}$ is the mass-center acceleration of the elevator, which is given by the gravitational acceleration

at the mass-center position r_e of the elevator, $\boldsymbol{g} = \nabla(GM/r_e)$. Therefore, in this frequency shift, the first order Doppler term becomes $-g\Delta r/c^2$ with order of c^{-2} and the second Doppler effect reduces to the order of c^{-3}. We can re-express frequency shift (1) as

$$\frac{f_B}{f_A} - 1 = \frac{1}{c^2}\left(\frac{GM}{r_B} - \frac{GM}{r_A} - \delta r \boldsymbol{n}_{AB} \cdot \nabla\frac{GM}{r_e}\right), \tag{2}$$

which can represent the experimental outcome and the terms inside the parentheses represent the difference in tidal potentials. Clearly, the clock-comparison result comes from the difference in tidal potentials between clock A and clock B, and the classic gravitational redshift effect due to a massive body is not displayed. In the case of a uniform gravitational field, the gravitational redshift term and Doppler term will cancel out completely, and the experimental outcome is independent of the external gravitational field. It can be inferred that the two clocks fixed in the freely falling *elevator* do not display a frequency difference due to external masses at first order in $\Delta U/c^2$ (U is the Newtonian potential of external masses). This is an important consequence of equivalence principle.

2.2. Clock Comparison in the Barycentric Coordinate Reference System

Here, we consider the outcome of s clock comparison experiment in the vicinity of the Earth, which can be precisely described in both BCRS and GCRS. The BCRS is a particular implementation of the barycentric reference system of the solar system, which has its origin at the solar system barycenter. The clock comparison can be adequately described in the BCRS. The BCRS coordinates are set as $(ct, \mathbf{x})$. Therefore, we should study the frequency shift between clocks in the BCRS. To determine a one-way frequency shift between two clocks, we consider that clock A sends a signal with the proper frequency f_A and the same signal is received by clock B with the proper frequency f_B. The one-way frequency shift is then given by

$$\frac{f_A}{f_B} = \left(\frac{d\tau_B}{dt_B}\right)_{t_B}\left(\frac{dt_A}{d\tau_A}\right)_{t_A}\left(\frac{dt_B}{dt_A}\right), \tag{3}$$

where τ_A and τ_B are the proper time of clocks A and B, respectively. t_A and t_B are the coordinate times corresponding to proper times τ_A and τ_B.

The derivatives $d\tau_A/dt_A$ and $d\tau_B/dt_B$ depend on the state of clocks containing the gravitational redshift and second-order Doppler effect. They may be calculated by using the invariance of the Riemannian spacetime interval. Considering a clock, the invariable spacetime interval is given by

$$ds^2 = g_{00}c^2dt^2 + 2g_{0i}cdtdx^i + g_{ij}dx^i dx^j = -c^2 d\tau^2. \tag{4}$$

Given a requirement of frequency shift, it allows us to calculate the gravitational contributions to the corresponding accuracy due to the Earth's Newtonian gravitational potential, Earth's mass multipole moments and external masses' gravitational potential.

The term dt_A/dt_B is dependent on a light trajectory of the signal. For example, for clock-comparison experiments with optical fiber links, light trajectory depends on optical fiber. Clearly, this term includes influences of changing refractive index, changing fiber length due to temperature and effects due to fiber motion, etc. These influences have been investigated in detail [42,43]. Furthermore, it is not our purpose in this paper to study them.

To develop Equation (3), we consider the metric tensor. With the recommendations of the International Astronomical Union (IAU) resolutions (IAU Resolution B1.3 (2000)) [5], the metric tensor in the BCRS can be written in the form only of harmonic potentials

$$
\begin{aligned}
g_{00} &= -1 + \frac{2w}{c^2} + O(c^{-4}), \\
g_{0i} &= O(c^{-3}), \\
g_{ij} &= \delta_{ij}\left(1 + \frac{2w}{c^2}\right) + O(c^{-4}),
\end{aligned}
\tag{5}
$$

where w is a scalar potential. This form of metric tensor is now sufficient for most modern precision experiments of time and frequency foreseen in the next few years. The scalar potential w is given by the form

$$
w = w_0 + w_L = \sum_b \frac{GM_b}{r_b} + w_L,
\tag{6}
$$

where r_b is the barycentric position of body b and w_L represents contributions from higher gravitational potential coefficients. For most cases, it is sufficient to use the mass-monopole approximation ($w_L = 0$); however, this term should be kept to ensure consistency in all cases, such as experiments in the vicinity of Earth.

Then from Equations (4) and (5), the derivative term $d\tau/dt$ can be expressed as

$$
\frac{d\tau}{dt} = 1 - \frac{1}{c^2}\left(w + \frac{v^2}{2}\right) + O(c^{-4}).
\tag{7}
$$

For the influence of gravitational fields, it is reasonable to split Earth mass and external masses (the Sun, Moon and planets). The proper time of a clock A located on the surface of the Earth $\mathbf{x}_A(t)$ is given by

$$
\frac{d\tau_A}{dt} = 1 - \frac{1}{c^2}\left(w_{0,ext} + w_{0,E} + w_{L,E} + \frac{\mathbf{v}^2}{2}\right)_A,
\tag{8}
$$

where subscript A represents all quantities expressed for clock A, $w_{0,E}$ is the Newtonian gravitational potential of the Earth, $w_{0,ext}$ is the summation of Newtonian potential over all solar system bodies except Earth and $w_{L,E}$ contains Earth's mass multipole moments. For a clock on the surface of the Earth, it is desirable to separate the clock-dependent part and the clock-independent part from this equation. The barycentric coordinate and barycentric velocity can be written as $\mathbf{x}_A = \mathbf{x}_E + \mathbf{x}_{EA}$ and $\mathbf{v}_A = \dot{\mathbf{x}}_A + \dot{\mathbf{x}}_{EA}$, respectively. Then by using the Legendre polynomials, the scalar potential can be expressed as

$$
w_{0,ext}(\mathbf{x}_A) = \sum_{b \neq E} \frac{GM_b}{r_{bE}}\left[1 - \frac{\mathbf{x}_{bE} \cdot \mathbf{x}_{EA}}{r_{bE}^2} - \frac{\mathbf{x}_{EA}^2}{2r_{bE}^2} + \frac{3(\mathbf{x}_{bE} \cdot \mathbf{x}_{EA})^2}{2r_{bE}^4}\right] + O(r_{bE}^{-3}),
\tag{9}
$$

where r_{bE} is the distance between body b and the Earth. At the same time, the term $\mathbf{v}_A^2$ may be expressed using Earth-dependent quantities as

$$
\mathbf{v}_A^2 = \mathbf{v}_E^2 + 2\mathbf{v}_E \cdot \dot{\mathbf{x}}_{EA} + \dot{\mathbf{x}}_{EA}^2,
\tag{10}
$$

where the second term can be further expressed as the form

$$
\mathbf{v}_E \cdot \dot{\mathbf{x}}_{EA} = \frac{d}{dt}(\dot{\mathbf{x}}_E \cdot \mathbf{x}_{EA}) - \ddot{\mathbf{x}}_E \cdot \mathbf{x}_{EA}.
\tag{11}
$$

It is noted that the second-order Doppler effect contains an acceleration-dependent part. Clearly the Earth's acceleration in the barycentric celestial coordinate system is

$$\ddot{\mathbf{x}}_E = \nabla w_{0,ext} = \sum_{b \neq E} -\frac{GM_b}{r_{bE}^3} \mathbf{x}_{bE}. \tag{12}$$

From the expression of acceleration, it is clear that the second term in Equation (11) has the same form as but opposite sign to the second term on the right-hand side of Equation (9). It leads to an incredible cancellation.

Substituting Equations (9)–(12) into Equation (8), the c^{-2} term becomes

$$\frac{1}{c^2}\Big[\sum_{b \neq E} \frac{GM_b}{r_{bE}} + w_{0,E}(\mathbf{x}_{EA}) + w_{L,E}(\mathbf{x}_{EA}) + \frac{\mathbf{v}_E^2}{2} + \frac{\dot{\mathbf{x}}_{EA}^2}{2}$$

$$+ \sum_{b \neq E} \frac{GM_b r_{EA}^2}{2r_{bE}^3}(3(\mathbf{n}_{bE} \cdot \mathbf{n}_{EA})^2 - 1) + \frac{d}{dt}(\dot{\mathbf{x}}_E \cdot \mathbf{x}_{EA})\Big], \tag{13}$$

where $\mathbf{n}_{bE} = \mathbf{x}_{bE}/r_{bE}$, $\mathbf{n}_{EA} = \mathbf{x}_{EA}/r_{EA}$. The cancellation in the c^{-2} term due to the second term of Equation (9) and second term of Equation (10) is in accordance with the equivalence principle. The last term is a consequence of the different definitions of simultaneity between the barycentric and geocentric reference system. This difference is due to the relative velocity $\mathbf{v}_E$ between the two reference systems and can correctly be described by the Lorentz transformation [14]. However, here we present a more straightforward method to deduce it. We assume that two clocks are placed in the GCRS where clock A is placed on the origin of GCRS and another clock B is fixed in position $\mathbf{X}$. Considering the synchronization by Einstein procedure, a light signal is emitted by clock A with the reading $\tau_A = 0$ and the same signal is received by clock B with the reading τ_B. When $\tau_B = |\mathbf{X}|/c$, we think that two clocks are simultaneous in the GCRS. However, this situation is different in the BCRS because of the relativity of simultaneity. When these two clocks are simultaneous in the BCRS, we consider this physical procedure in BCRS. When the signal is received by clock B, the reading τ_B of the clock B in the BCRS should be

$$\tau_B = \frac{|\mathbf{r}|}{|\mathbf{c} - \mathbf{v}_E|} = \frac{r}{c} + \frac{\mathbf{v}_E \cdot \mathbf{r}}{c^2} + O(c^{-3}), \tag{14}$$

where the difference between $\mathbf{r}$ and $\mathbf{X}$ is the order of c^{-2}. The second term describes the different definitions of simultaneity between two reference systems.

By introducing an instantaneous coordinate distance $\mathbf{r}_{AB} = \mathbf{x}_B(t_A) - \mathbf{x}_A(t_A)$, the term dt_B/dt_A is

$$\frac{dt_B}{dt_A} = 1 + \frac{d}{dt_A}\Big[\frac{r_{AB}}{c} + \frac{\mathbf{r}_{AB} \cdot \mathbf{v}_B}{c^2}\Big], \tag{15}$$

where all the quantities are measured at emission instant time t_A and $\mathbf{v}_B$ is the velocity of clock B.

From Equation (3), we express the frequency shift between two clocks in BCRS as follows

$$\frac{f_A}{f_B} = 1 + \frac{d}{dt}\Big(\frac{r_{AB}}{c}\Big) + \frac{1}{c^2}\Big[\frac{\dot{\mathbf{x}}_{EA}^2}{2} - \frac{\dot{\mathbf{x}}_{EB}^2}{2} + w_{0,E}(\mathbf{x}_{EA}) - w_{0,E}(\mathbf{x}_{EB}) + w_{L,E}(\mathbf{x}_{EA}) - w_{L,E}(\mathbf{x}_{EB}) + \frac{d}{dt}[\dot{\mathbf{x}}_{EB} \cdot \mathbf{x}_{AB}]$$

$$+ \sum_{b \neq E} \frac{GM_b r_{EA}^2}{2r_{bE}^3}(3(\mathbf{n}_{bE} \cdot \mathbf{n}_{EA})^2 - 1) - \sum_{b \neq E} \frac{GM_b r_{EB}^2}{2r_{bE}^3}(3(\mathbf{n}_{bE} \cdot \mathbf{n}_{EB})^2 - 1)\Big]. \tag{16}$$

The last two terms represent contributions from the Sun, Moon and other planets (excluding the Earth). In the measurement of effects on clock comparison, the frequency observable does not reveal the frequency shift due to the Sun's and Moon's gravitational potentials at the first order, which is due to a wonderful cancellation from Equations (9) and (10). This cancellation is intrinsic and is an important result of the equivalence principle. From

Equation (16), the Sun's and Moon's gravitational effects come from inhomogeneities of the gravitational field, in other words, tidal effects. Clock comparisons in the vicinity of the Earth cannot test the classic gravitational redshift of the Sun and Moon.

2.3. Clock Comparison in the Geocentric Coordinate Reference System

The origin of GCRS is the mass center of Earth. The GCRS is physically adequate to describe processes occurring in the vicinity of Earth. For most of the experiments in the vicinity of Earth, adopting GCRS is more convenient for the calculations of observable modeling. The GCRS coordinates are set as $(cT, \mathbf{X})$. With the recommendations of IAU resolutions (IAU Resolution B1.3 (2000)) [5], the metric tensor in GCRS may be also written as

$$
\begin{aligned}
G_{00} &= -1 + \frac{2W}{c^2} + O(c^{-4}), \\
G_{0i} &= O(c^{-3}), \\
G_{ij} &= \delta_{ij}\left(1 + \frac{2W}{c^2}\right) + O(c^{-4}),
\end{aligned}
\tag{17}
$$

where W is the scalar harmonic potential, which may be written as

$$
W = W_E + W_{ext} + O(c^{-4}),
\tag{18}
$$

where *ext* represents the contribution from external bodies. In the vicinity of the Earth, it is advantageous to express the Earth's gravitational potential W_E as multipole series that are usually called potential coefficients or Blanchet–Damour (B–D) moments. Blanchet–Damour (B–D) moments contain the contributions from the higher gravitational potential of the Earth ($w_{L.E}$ term in BCRS). Then, another term, external potential W_{ext}, is given by

$$
W_{ext} = W_{tidal} + W_{iner}.
\tag{19}
$$

The W_{iner} term is linear in the four-acceleration term of the geocenter, which vanishes for a purely spherical and nonrotating Earth. This term is small enough for the current clocks. The tidal potential W_{tidal} is given by the term of the Newtonian contributions (primarily due to the Sun and Moon)

$$
\begin{aligned}
W_{tidal} &= \sum_{b \neq E}\left[U_b(\mathbf{r}_{bE} + \mathbf{X}) - U_b(\mathbf{r}_{bE}) - \mathbf{X} \cdot \nabla U_b(\mathbf{r}_{bE})\right] \\
&= \sum_{b \neq E}\frac{GM_b}{2r_{bE}^3}\left[3(\mathbf{n}_{bE} \cdot \mathbf{X})^2 - \mathbf{X}^2\right] + O(r_{bE}^{-4}),
\end{aligned}
\tag{20}
$$

where $\mathbf{X}$ is the position in GCRS and U_b is the Newtonian gravitational potential of body b.

By using the same method of BCRS, the proper time of a clock A located on the surface of the Earth $\mathbf{X}_A(t)$ is given by

$$
\frac{d\tau_A}{dT} = 1 - \frac{1}{c^2}\left(W_E + W_{tidal} + \frac{V^2}{2}\right)_A
\tag{21}
$$

where V is the geocentric velocity of clock A and subscript A represents all quantities expressed for clock A.

Furthermore, introducing an instantaneous geocentric coordinate distance $\mathbf{R}_{AB} = \mathbf{X}_B(T_A) - \mathbf{X}_A(T_A)$, the term dT_B/dT_A is given using the quantities measured at emission instant T_A as

$$
\frac{dT_B}{dT_A} = 1 + \frac{d}{dT_A}\left(\frac{R_{AB}}{c} + \frac{\mathbf{R}_{AB} \cdot \mathbf{V}_B}{c^2}\right),
\tag{22}
$$

where $\mathbf{V}_B$ is the geocentric velocity of clock B.

After the above manipulations, we can express the frequency shift between two clocks from Equation (3) in the GCRS

$$
\begin{aligned}
\frac{f_A}{f_B} =\; & 1 + \frac{dR_{AB}}{cdT} + \frac{1}{c^2}\Big[\frac{\dot{\mathbf{X}}_A^2}{2} - \frac{\dot{\mathbf{X}}_B^2}{2} + W_E(\mathbf{X}_A) - W_E(\mathbf{X}_B) - \frac{d}{dT}\Big(\dot{\mathbf{X}}_B \cdot \mathbf{X}_{AB}\Big) \\
& + \sum_{b \neq E} \frac{GM_b X_A^2}{2r_{bE}^3}(3(\mathbf{n}_{bE}\cdot\mathbf{N}_A)^2 - 1) - \sum_{b \neq E} \frac{GM_b X_B^2}{2r_{bE}^3}(3(\mathbf{n}_{bE}\cdot\mathbf{N}_B)^2 - 1)\Big].
\end{aligned}
\tag{23}
$$

The calculation of frequency shift in BCRS is straightforwardly obtained with a simpler procedure where every term has definite physical meanings. Clearly, the results of frequency shifts (16) and (23) are identical. It points out again that clock comparison does not display the frequency shift caused by the Sun's and Moon's gravitational potentials at the first order $\Delta U_{S/M}/c^2$. Therefore we can conveniently adopt GCRS for the modeling of a clock experiment in the vicinity of Earth. For clock comparisons, the absolute measurement of influence of the Sun and Moon masses is tidal effects. A rough estimation demonstrates that relativistic tidal effects (Sun's and Moon's gravitational effects) can reach the level of 10^{-18} for several-100 km clock-comparison experiments on the surface of Earth, which motivates a test of tidal effect with clock comparisons.

3. Experimental Estimation for Tidal Effects

For the measurement and test of tidal effects, we estimate the available accuracy with some clock experiments. Firstly, we consider clock comparisons in laboratories. As mentioned above, the tidal potentials of the Sun and Moon change the rates of clocks. Except for the tidal potentials of the Sun and Moon, the tidal response of solid Earth is also nonnegligible for clock comparisons with long distances. Due to the Earth's elasticity, tidal forces produce the deformations in the solid Earth and ocean, and the changes of the density of the solid Earth. These influences can be studied by the Love numbers. Taking tidal potentials of the Sun and Moon and the tidal response of solid Earth into account, the tidal effects on clock comparisons in laboratories can be expressed as

$$
\left(\frac{\Delta f}{f}\right)_{tidal,g} = \frac{1 - h_2 + k_2}{c^2}\sum_{b \neq E}\frac{GM_b}{2r_{bE}^3}\Big[\big(3(\mathbf{n}_{bE}\cdot\mathbf{X}_A)^2 - \mathbf{X}_A^2\big) - \big(3(\mathbf{n}_{bE}\cdot\mathbf{X})_B^2 - \mathbf{X}_B^2\big)\Big],
\tag{24}
$$

where $\mathbf{X}_{A/B}$ represents the position vector of the laboratory on the Earth, and h_2 and k_2 are the Love numbers describing the deformations of the Earth and Earth mass redistribution, respectively. From an estimation of this equation, tidal effects lead to a periodic signal of around 1×10^{-17} peak to peak for clock or frequency comparisons with distances $\sim$1000 km. This is a measurable signal for current clocks.

For estimating tidal effects in space missions, we consider the tidal influences on the satellite clock. Considering an in-orbit clock, the influences of the tidal potentials of the Sun and Moon and the tidal response of solid Earth are given by

$$
\left(\frac{\delta f}{f}\right)_{tidal,s} = \sum_{b \neq E}\frac{GM_b R^2}{2c^2 r_{bE}^3}\Big[3(\mathbf{n}_{bE}\cdot\mathbf{N})^2 - 1\Big] + k_2\frac{R_{0E}^5}{c^2 R^3}\sum_{b \neq E}\frac{GM_b}{2r_{bE}^3}\Big[3(\mathbf{n}_{bE}\cdot\mathbf{N})^2 - 1\Big],
\tag{25}
$$

where R is the distance between the center of mass of the Earth and the satellite, R_{0E} is the equatorial radius of Earth, and $\mathbf{N}$ is the unit vector pointing from the center of mass of the Earth to the satellite. The first and second terms are the contributions from Sun's and Moon's tidal potentials and tidal response of solid Earth, respectively. With the satellite's altitudes increasing, the tidal effects due to the Sun's and Moon's masses increase quadratically and the tidal effect due to the tidal response of solid Earth decays cubically. For an in-orbit clock, the influence of tidal effects mainly comes from the first term.

To demonstrate tidal effects on clock experiments, we simulate the clock comparison between two locations, $\mathcal{A}$ and $\mathcal{B}$. The geographic location information is that the east

longitude and north latitude of $\mathcal{A}$ are E114° and N30° (Wuhan), and that of $\mathcal{B}$ are E116° and N40° (Beijing), respectively. The distance between $\mathcal{A}$ and $\mathcal{B}$ is about 1100 km. We shall use nominal planetary ephemeris, astronomy parameters, gravitational constants of Earth, Sun and Moon, etc. Figure 1 shows the calculated fractional frequency shift due to the tidal potentials between $\mathcal{A}$ and $\mathcal{B}$, and the date begins from 1 January 2024 with a total time of 720 h. From the figure, tidal effects on clock comparison present an obvious periodic signal with around 1×10^{-17} peak to peak. The measurement of this effect is achievable for modern clock experiments. Considering a feasible experiment, the $\mathcal{A}$ and $\mathcal{B}$ perform clock comparisons with frequency instability of $1 \times 10^{-16} \, \tau^{-1/2}$. After an observation time of 60 days, a test of tidal effects on clock comparison can reach the level of 1%. Considering the clock-comparison experiment in the Tokyo Tower [3], the tidal effects lead to only a fractional frequency shift with an order of 10^{-21}, which can be negligible for current clocks. From Equation (24), the tidal effects are more significant for clocks with greater distances or height differences. However, for the current clock comparison experiment with tower, measuring the tidal effects requires the accuracy and stability of the clocks to reach a level of 10^{-20} or 10^{-21}.
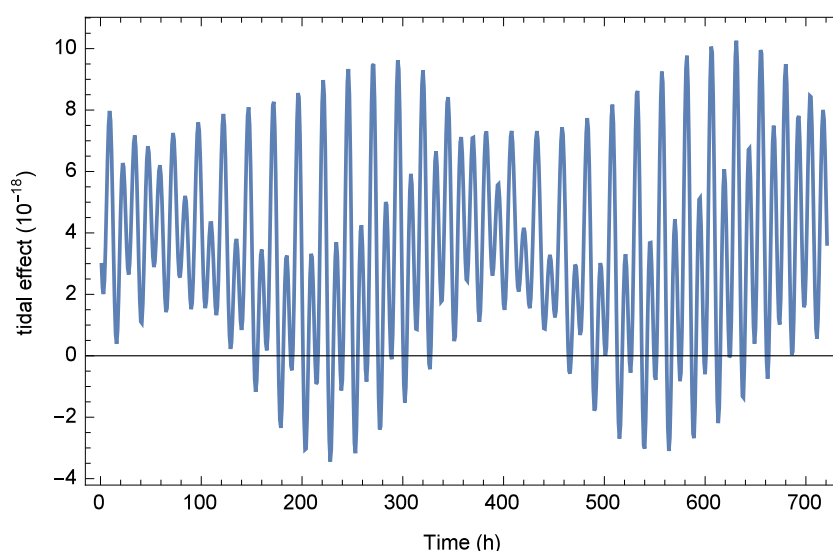

Figure 1. The calculated frequency shift for a clock comparison in laboratory. The curve represents the fractional frequency shift between $\mathcal{A}$ (E114°, N30°) and $\mathcal{B}$ (E1116°, N40°) due to tidal potentials.

From the first term of Equation (25), the tidal effects due to the Sun and Moon masses increase quadratically with distance from the Earth's center of mass; then the international missions with in-orbit clocks around the Earth may have more potential to test tidal effects. Another advantage is that the influence of Earth solid tides is much smaller for in-orbit clocks. The China space station has recently been launched with an orbital height about 400 km. It will demonstrate an optical atomic clock in coming years whose long-term stability is 8×10^{-18} [44]. For a running time of 60 days, it can test tidal effects to the level of 10%, which is mainly limited by the instability of the clocks. Figure 2 shows the calculated frequency shift due to the tidal potentials on clock comparison between $\mathcal{B}$ and China space station. The tidal effects lead to a periodic signal about 3×10^{-17} peak to peak. For clocks of Galileo satellites, tidal effects due to the Sun and Moon masses can lead to a periodic signal of around 12 ps peak to peak, which may be visible for improved accuracy. The FOCOS mission aims to deploy a state-of-the-art optical clock with a long-term stability of 1×10^{-18} and laser links in space [37]. With an orbital altitude around 10,000 km, tidal effects are more significant. These advantages make this mission to test tidal effects with an accuracy of 0.3%.
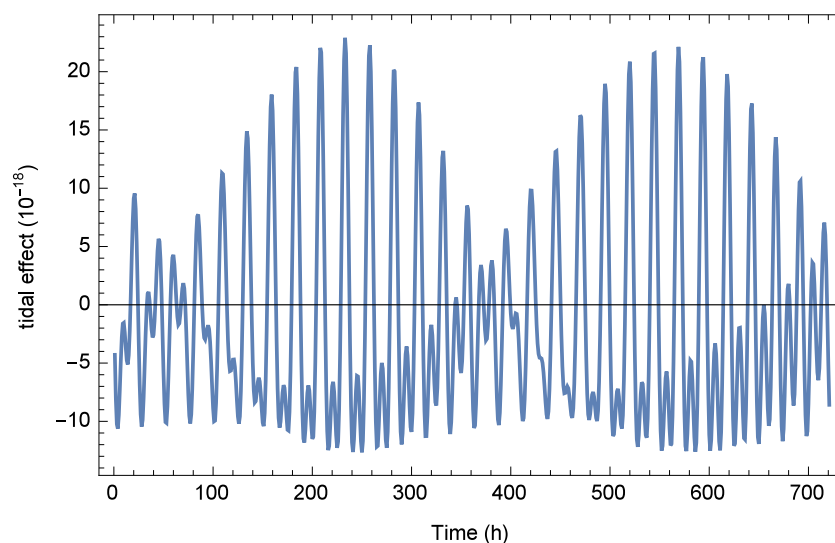
Figure 2. The calculated frequency shift for a clock comparison between laboratory and space. The curve represents the fractional frequency shift between the $\mathcal{B}$ clock and the China space station clock due to tidal potentials.

4. Conclusions

In this work, we present a relativistic procedure to rigorously deduce the algorithms of frequency shift in the framework of general relativity that include scenarios in the BCRS and GCRS. In the BCRS, gravitational redshift and Doppler effects cancel each other for clock experiments in the vicinity of Earth, so they do not have measurable physical observables. From the equivalence principle, this cancellation is intrinsic. For the clock comparisons in these experiments, it does not display a frequency shift due to the Sun's and Moon's gravitational potentials at the first order $\Delta U_{S/M}/c^2$, and the influence of the Sun's and Moon's masses is presented in the form of tidal potential. The same clock experiment can be described in the GCRS with a simpler mathematical form and definite physical meaning. The gravitational redshift with the Earth mass is a classic test and has been validated with high precision. For the Sun and Moon masses, the measurement of tidal effects on clock experiments is a test of a different aspect of general relativity.

Benefiting from high-precision atomic clocks and optical links, the frequency shift due to tidal effects can be measured in experiments reaching the level of 10^{-17} for clock comparisons with the distance $\sim$1000 km. The estimations of testing tidal effect are presented with different experiments or projects. The calculation demonstrates that clock-comparison experiments with a distance of 1100 km can test tidal effects to the level of 1%, where an observation time of 60 days is needed. The China space station can test tidal effects with a level of 10% with optical clocks. The more promising FOCOS mission using the state-of-the-art optical clock in space may test tidal effects to an accuracy of 3×10^{-3}. As the influence of external mass in a freely falling frame, it is also necessary to validate the tidal effects of the Sun and Moon in clock-comparison experiments.

Author Contributions: Conceptualization, C.-G.Q. and C.-G.S.; Writing-original draft, C.-G.Q.; Writing—review and editing, C.-G.Q., Y.-J.T. and C.-G.Q.; Software, C.-G.Q. and J.-Z.D.; Investigation, X.-Y.D.; Resources, T.L.; Validation, Y.-J.T.; Supervision, C.-G.S. All authors have read and agreed to the published version of the manuscript.

Data Availability Statement: No data were used to support this study.

References

1. Delva, P.; Puchades, N.; Schönemann, E.; Dilssner, F.; Courde, C.; Bertone, S.; Gonzalez, F.; Hees, A.; Poncin-Lafitte, C.L.; Meynadier, F.; et al. Gravitational redshift test using eccentric Galileo satellites. *Phys. Rev. Lett.* **2018**, *121*, 231101. [CrossRef] [PubMed]
2. Herrmann, S.; Finke, F.; Lülf, M.; Kichakova, O.; Puetzfeld, D.; Knickmann, D.; List, M.; Rievers, B.; Giorgi, G.; Günther, C.; et al. Test of the gravitational redshift with Galileo satellites in an eccentric orbit. *Phys. Rev. Lett.* **2018**, *121*, 231102. [CrossRef] [PubMed]
3. Takamoto, M.; Ushijima, I.; Ohmae, N.; Yahagi, T.; Kokado, K.; Shinkai, H.; Katori, H. Test of general relativity by a pair of transportable optical lattice clocks. *Nat. Photonics* **2020**, *14*, 411–415. [CrossRef]
4. Poisson, E.; Will, C.M. *Gravity: Newtonian, Post–Newtonian, Relativistic*; Cambridge University Press: Cambridge, UK, 2014.
5. Soffel, M.; Klioner, S.A.; Petit, G.; Wolf, P.; Kopeikin, S.M.; Bretagnon, P.; Brumberg, V.A.; Capitaine, N.; Damour, T.; Fukushima, T.; et al. The IAU 2000 Resolutions for Astrometry, Celestial Mechanics, and Metrology in the Relativistic Framework: Explanatory Supplement. *Astrophys. J.* **2003**, *126*, 2687. [CrossRef]
6. Qin, C.G.; Tan, Y.J.; Shao, C.G. Relativistic tidal effects on clock-comparison experiments. *Class. Quantum Grav.* **2019**, *36*, 055008. [CrossRef]
7. Qin, C.G.; Tan, Y.J.; Shao, C.G. The Tidal Clock Effects of the Lunisolar Gravitational Field and the Earth's Tidal Deformation. *Astron. J.* **2020**, *160*, 272. [CrossRef]
8. Hinkley, N.; Sherman, J.A.; Phillips, N.B.; Schioppo, M.; Lemke, N.D.; Beloy, K.; Pizzocaro, M.; Oates, C.W.; Ludlow, A.D. An atomic clock with 10^{-18} instability. *Science* **2013**, *341*, 1215–1218. [CrossRef]
9. Bloom, B.J.; Nicholson, T.L.; Williams, J.R.; Campbell, S.L.; Bishof, M.; Zhang, X.; Zhang, W.; Bromley, S.L.; Ye, J. An optical lattice clock with accuracy and stability at the 10^{-18} level. *Nature* **2014**, *506*, 71–75. [CrossRef]
10. Nicholson, T.L.; Campbell, S.L.; Hutson, R.B.; Marti, G.E.; Bloom, B.J.; McNally, R.L.; Zhang, W.; Barrett, M.D.; Safronova, M.S.; Strouse, G.F.; et al. Systematic evaluation of an atomic clock at 2×10^{-18} total uncertainty. *Nat. Commun.* **2015**, *6*, 6896. [CrossRef]
11. Delva, P.; Lodewyck, J.; Bilicki, S.; Bookjans, E.; Vallet, G.; Le Targat, R.; Pottie, P.-E.; Guerlin, C.; Meynadier, F.; Le Poncin-Lafitte, C.; et al. Test of Special Relativity Using a Fiber Network of Optical Clocks. *Phys. Rev. Lett.* **2017**, *118*, 221102. [CrossRef]
12. McGrew, W.F.; Zhang, X.; Fasano, R.J.; Schäffer, S.A.; Beloy, K.; Nicolodi, D.; Brown, R.C.; Hinkley, N.; Milani, G.; Schioppo, M.; et al. Atomic clock performance enabling geodesy below the centimetre level. *Nature* **2018**, *564*, 87–90. [CrossRef]
13. Beloy, K.; Bodine, M.I.; Bothwell, T.; Brewer, S.M.; Bromley, S.L.; Chen, J.-S.; Deschênes, J.-D.; Diddams, S.A.; Fasano, R.J.; Fortier, T.M.; et al. Frequency ratio measurements with 18-digit accuracy using a network of optical clocks. *Nature* **2021**, *591*, 564–569.
14. Nelson, R.A. Relativistic time transfer in the vicinity of the Earth and in the solar system. *Metrologia* **2011**, *48*, S171–S180. [CrossRef]
15. Jaduszliwer, B.; Camparo, J. Past, present and future of atomic clocks for GNSS. *GPS Solut.* **2021**, *25*, 1–13. [CrossRef]
16. Grotti, J.; Koller, S.; Vogt, S.; Häfner, S.; Sterr, U.; Lisdat, C.; Denker, H.; Voigt, C.; Timmen, L.; Rolland, A.; et al. Geodesy and metrology with a transportable optical clock. *Nat. Phys.* **2018**, *14*, 437–441. [CrossRef]
17. Müller, J.; Soffel, M.; Klioner, S.A. Geodesy and Relativity. *J. Geod.* **2008**, *82*, 133–145. [CrossRef]
18. Kouvaris, C.; Papantonopoulos, E.; Street, L.; Wijewardhana, L.C.R. Using atomic clocks to detect local dark matter halos. *Phys. Rev. D* **2021**, *104*, 103025. [CrossRef]
19. Kobayashi, T.; Takamizawa, A.; Akamatsu, D.; Kawasaki, A.; Nishiyama, A.; Hosaka, K.; Hisai, Y.; Wada, M.; Inaba, H.; Tanabe, T.; et al. Search for ultralight dark matter from long-term frequency comparisons of optical and microwave atomic clocks. *Phys. Rev. Lett.* **2022**, *129*, 241301. [CrossRef]
20. Antypas, D.; Tretiak, O.; Garcon, A.; Ozeri, R.; Perez, G.; Budker, D. Scalar dark matter in the radio-frequency band: Atomic-spectroscopy search results. *Phys. Rev. Lett.* **2019**, *123*, 141102. [CrossRef]
21. Roberts, B.M.; Derevianko, A. Precision measurement noise asymmetry and its annual modulation as a dark matter signature. *Universe* **2021**, *7*, 50. [CrossRef]
22. Sanner, C.; Huntemann, N.; Lange, R.; Tamm, C.; Peik, E.; Safronova, M.S.; Porsev, S.G. Optical clock comparison for Lorentz symmetry testing. *Nature* **2019**, *567*, 204–208. [CrossRef] [PubMed]
23. Hees, A.; Bailey, Q.G.; Bourgoin, A.; Pihan-Le Bars, H.; Guerlin, C.; Le Poncin-Lafitte, C. Tests of Lorentz symmetry in the gravitational sector. *Universe* **2016**, *2*, 30. [CrossRef]
24. Wolf, P.; Chapelet, F.; Bize, S.; Clairon, A. Cold atom clock test of Lorentz invariance in the matter sector. *Phys. Rev. Lett.* **2006**, *96*, 060801. [CrossRef] [PubMed]
25. Qin, C.G.; Tan, Y.J.; Shao, C.G. Test of Einstein Equivalence Principle by frequency comparisons of optical clocks. *Phys. Lett. B* **2021**, *820*, 136471. [CrossRef]

26. Godun, R.M.; Nisbet-Jones, P.B.R.; Jones, J.M.; King, S.A.; Johnson, L.A.M.; Margolis, H.S.; Szymaniec, K.; Lea, S.N.; Bongs, K.; Gill, P. Frequency Ratio of Two Optical Clock Transitions in ^{171}Yb$^+$ and Constraints on the Time Variation of Fundamental Constants. *Phys. Rev. Lett.* **2014**, *113*, 210801. [CrossRef]

27. Huntemann, N.; Lipphardt, B.; Tamm, C.; Gerginov, V.; Weyers, S.; Peik, E. Improved Limit on a Temporal Variation of m_p/m_e from Comparisons of Yb$^+$ and Cs Atomic Clocks. *Phys. Rev. Lett.* **2014**, *113*, 210802. [CrossRef]

28. Lange, R.; Huntemann, N.; Rahm, J.M.; Sanner, C.; Shao, H.; Lipphardt, B.; Tamm, C.; Weyers, S.; Peik, E. Improved limits for violations of local position invariance from atomic clock comparisons. *Phys. Rev. Lett.* **2021**, *126*, 011102. [CrossRef]

29. Kostelecký, A. The search for relativity violations. *Sci. Am.* **2004**, *291*, 92–101. [CrossRef]

30. Bluhm, R.; Kostelecký, V.A.; Lane, C.D.; Russell, N. Probing Lorentz and CPT violation with space-based experiments. *Phys. Rev. D* **2003**, *68*, 125008. [CrossRef]

31. Kostelecký, V.A.; Vargas, A.J. Lorentz anD CPT tests with clock-comparison experiments. *Phys. Rev. D* **2018**, *98*, 036003. [CrossRef]

32. Bluhm, R.; Kostelecký, V.A.; Lane, C.D.; Russell, N. Clock-comparison tests of Lorentz and CPT symmetry in space. *Phys. Rev. Lett.* **2002**, *88*, 090801. [CrossRef]

33. Pihan-Le Bars, H.; Guerlin, C.; Lasseri, R.-D.; Ebran, J.-P.; Bailey, Q.; Bize, S.; Khan, E.; Wolf, P. Lorentz-symmetry test at Planck-scale suppression with nucleons in a spin-polarized ^{133}Cs cold atom clock. *Phys. Rev. D* **2017**, *95*, 075026. [CrossRef]

34. Aguilera, D.N.; Ahlers, H.; Battelier, B.; Bawamia, A.; Bertoldi, A.; Bondarescu, R.; Bongs, K.; Bouyer, P.; Braxmaier, C.; Cacciapuoti, L.; et al. STE-QUEST-test of the universality of free fall using cold atom interferometry. *Class. Quantum Gravity* **2014**, *31*, 115010. [CrossRef]

35. Savalle, E.; Guerlin, C.; Delva, P.; Meynadier, F.; le Poncin-Lafitte, C.; Wolf, P. Gravitational redshift test with the future ACES mission. *Class. Quantum Gravity* **2019**, *36*, 245004. [CrossRef]

36. Liu, L.; Lü, D.-S.; Chen, W.-B.; Li, T.; Qu, Q.-Z.; Wang, B.; Li, L.; Ren, W.; Dong, Z.-R.; Zhao, J.-B.; et al. In-orbit operation of an atomic clock based on laser-cooled 87Rb atoms. *Nat. Commun.* **2018**, *9*, 2760. [CrossRef]

37. Derevianko, A.; Gibble, K.; Hollberg, L.; Newbury, N.R.; Oates, C.; Safronova, M.S.; Sinclair, L.C.; Yu, N. Fundamental physics with a state-of-the-art optical clock in space. *Quantum Sci. Technol.* **2022**, *7*, 044002. [CrossRef]

38. Droste, S.; Ozimek, F.; Udem, T.; Predehl, K.; Hänsch, T.W.; Schnatz, H.; Grosche, G.; Holzwarth, R. Optical-frequency transfer over a single-span 1840 km fiber link. *Phys. Rev. Lett.* **2013**, *111*, 110801. [CrossRef]

39. Turyshev, S.G.; Toth, V.T.; Sazhin, M.A. General relativistic observables of the GRAIL mission. *Phys. Rev. D* **2013**, *87*, 024020. [CrossRef]

40. Damour, T.; Soffel, M.; Xu, C.M. General-relativistic celestial mechanics. I. Method and definition of reference systems. *Phys. Rev. D* **1991**, *43*, 3273. [CrossRef]

41. Hoffmann, B. Noon-midnight red shift. *Phys. Rev.* **1961**, *121*, 337. [CrossRef]

42. Geršl, J.; Delva, P.; Wolf, P. Relativistic corrections for time and frequency transfer in optical fibres. *Metrologia* **2005**, *52*, 552–564. [CrossRef]

43. Cohen, L.G.; Fleming, J.W. Effect of temperature on trasmission in lightguides. *Bell Syst. Tech. J.* **1979**, *58*, 945–951. [CrossRef]

44. Shen, W.; Zhang, P.; Shen, Z.; Xu, R.; Sun, X.; Ashry, M.; Ruby, A.; Xu, W.; Wu, K.; Wu, Y.; et al. Testing gravitational redshift base on microwave frequency links onboard China Space Station. *arXiv* **2021**, arXiv:2112.02759.